ANTIOXIDANTS & REDOX SIGNALING
Volume 8, Numbers 7 & 8, 2006
© Mary Ann Liebert, Inc.

Original Research Communication

Role of Oxidative/Nitrosative Stress in the Tolerance to Ischemia/Reperfusion Injury in Cardiomyopathic Hamster Heart

SHIORI KYOI, HAJIME OTANI, SEIJI MATSUHISA, YUZO AKITA, CHIHARU ENOKI, KIMIKO TATSUMI, REIJI HATTORI, HIROJI IMAMURA, HIROSHI KAMIHATA, and TOSHIJI IWASAKA

ABSTRACT

We investigated the role of oxidative/nitrosative stress in the tolerance to ischemia/reperfusion (I/R) injury in BIO14.6 cardiomyopathy hamster hearts at 6 weeks of age. These hearts showed no significant morphologic change and left ventricular (LV) dysfunction. However, expression and activity of iNOS, nitrotyrosine (NT) formation, and protein kinase C (PKC)-ϵ activity were increased in these hearts. When the BIO14.6 hamster hearts were isolated and subjected to 40 min of global ischemia, they showed smaller myocardial necrosis and greater recovery of LV function during reperfusion compared with the control hamster heart. All of these effects were abrogated by prolonged treatment with the antioxidant, 2-mercaptopropionylglycine (MPG). Brief preischemic treatment with MPG or the iNOS inhibitor 1400W also abrogated NT formation and activation of PKC-ϵ and inhibited the tolerance to I/R injury in the BIO14.6 hamster heart. Brief preischemic treatment with the PKC inhibitor chelerythrine or the K_{ATP} channel blockers, 5-hydroxydecanoate (5-HD) and glibenclamide, had no effect on iNOS activation and NT formation but inhibited the tolerance to I/R injury in the cardiomyopathic heart. These results suggest that oxidative/nitrosative stress plays a role in the tolerance to I/R injury in the cardiomyopathic heart through activation of PKC and the downstream effectors, K_{ATP} channels. *Antioxid. Redox Signal.* 8, 1351–1361.

INTRODUCTION

OXIDATIVE/NITROSATIVE STRESS is increased in the heart under various pathologic such as inflammation, hypertension, and cardiomyopathy (22). Enhanced oxidative/nitrosative stress through the formation of peroxynitrite results in myocyte hypertrophy and apoptotic and necrotic death of myocytes that are responsible for the development of heart failure (31, 34, 37).

A growing body of evidence indicates that reactive oxygen species (ROS) play a crucial role in the acquisition of tolerance to ischemia/reperfusion (I/R) injury, as exemplified by ischemic preconditioning (30). Ischemic preconditioning was originally reported by Murry *et al*. (27), who demonstrated that cyclic episodes of a brief period of ischemia and reperfusion rendered the heart tolerant to subsequent lethal I/R injury for several hours. Recently, it has been revealed that ROS, in conjunction with nitric oxide (NO) generated during the preconditioning stimulus, activate cardioprotective signal transduction in this early preconditioning (26, 30). Preconditioning-induced generation of ROS and NO also triggers development of late preconditioning, which emerges at 12–24 h after the initial preconditioning challenge and lasts for approximately 48 h (19, 24). Although recent studies pointed to the obligatory role of inducible form of NO synthase (iNOS) to mediate late preconditioning (3, 4, 33), the role of ROS in the mediator phase of late preconditioning has not been determined. Similarly, the role of oxidative/nitrosative stress in the tolerance to I/R injury in pathologic hearts has not been studied. Accordingly, we used cardiomyopathic hamster heart to

Cardiovascular Center, Kansai Medical University, Moriguchi City, Japan.

examine the role of oxidative/nitrosative stress in the tolerance to I/R injury in this pathologic heart.

MATERIALS AND METHODS

Animals

Male BIO14.6 hamsters devoid of δ-sarcoglycan gene (28) and the control BIOF1B hamsters at 5 weeks of age were obtained from BIO Breeders (Fitchburg, MA) and housed under controlled temperature and humidity conditions. All experiments were conducted in accordance with the *Guidelines for the Care and Use of Laboratory Animals* (NIH publication No. 85–23, revised 1996) and approved by the Kansai Medical University Institutional Animal Care and Use Committee.

Echocardiography

At 6 weeks of age, the hamster was anesthetized intraperitoneally with a mixture of ketamine, xylazine, and acepromazine, as described (35). Echocardiography was performed by using a SONOS-7500 (Philips Medical Systems, Andover, MA) equipped with a 6- to 15-MHz transducer (model 21390A; Philips). M-mode measurements of left ventricular (LV) internal diameter were made from more than three beats and averaged. Measurements of the LV end-diastolic diameter were taken at the time of the apparent maximal LV diastolic dimension, whereas measurements of the LV end-systolic diameter were taken at the time of the most anterior systolic excursion of the posterior wall. LV ejection fraction was calculated according to the cubed method, as described (35).

Histological analysis

After echocardiography, the hamsters were anesthetized intraperitoneally with a lethal dose of pentobarbital sodium, and the chest was opened. The ascending aorta was cannulated with a 24-gauge catheter, and the heart was perfusion-fixed with 10% formalin, embedded in paraffin, and sectioned at 6-μm thickness. The section was stained with hematoxylin-eosin, and gross morphology of the heart was viewed under a low-power field (×0.5). The area of fibrosis was identified by Masson trichrome staining and was quantified by using image-analyzing software Win Roof (Mitani Co., Fukui, Japan).

Perfusion techniques

The hamsters were anesthetized intraperitoneally with a lethal dose (100 mg/kg) of pentobarbital sodium. The heart was excised, mounted on a Langendorff's perfusion apparatus, and perfused at a constant mean pressure of 70–75 mm Hg by using a Krebs–Henseleit bicarbonate (KHB) buffer solution of the following composition (in m*M*): 118 NaCl, 4.7 KCl, 1.2 $MgSO_4$, 25 $NaHCO_3$, 1.2 KH_2PO_4, 1.8 $CaCl_2$, and 11 glucose; pH 7.4 at 37°C, when equilibrated with a mixture of 95% O_2/5% CO_2 gas.

Isovolumic LV pressure measurements

Isovolumic LV function was monitored by using a compliant latex balloon–tipped catheter inserted into the LV through the left atrium and connected to a pressure transducer placed at equivalent height to the heart. The balloon was filled with saline to produce a LV end-diastolic pressure (LVEDP) of 5–10 mm Hg. Hemodynamic data were analyzed by using a Biomedical Research System (LEG-1000; Nihon Kohden, Osaka, Japan). Coronary flow was measured by timed collection of the coronary effluent.

Drugs

The antioxidant, *N*-(2-mercaptopropionyl)-glycine (MPG), the PKC inhibitor, chelerythrine, and the nonselective K_{ATP} channel blocker, glibenclamide, were purchased from Sigma Chemical (Tokyo, Japan). The iNOS-selective inhibitor, 1400W, was obtained from Alexis (San Diego, CA). The mitochondrial K_{ATP} (mitoK_{ATP}) channel blocker, 5-hydroxydecanoate (5-HD), was obtained from Biomol Research Labs, Inc. (Plymouth Meeting, PA). Chelerythrine, 1400W, 5-HD, and glibenclamide were dissolved in dimethylsulfoxide (DMSO) at a final concentration of 0.01%.

Experimental protocol

Experimental protocol is shown in Fig. 1. The control and BIO14.6 hamster hearts were subjected to 40 min of global ischemia followed by 120 min of reperfusion. In a chronic MPG group, MPG (100 mg/kg/day) dissolved in 0.2 ml PBS was injected intraperitoneally for 5 days, and the heart was excised 24 h after the last administration of MPG. All other groups received the same amount of PBS intraperitoneally for 5 days. Preischemic treatment groups received 0.3 m*M* MPG, 10 μ*M* 1400W, 5 μ*M* chelerythrine, 0.5 m*M* 5-HD, or 10 μ*M*

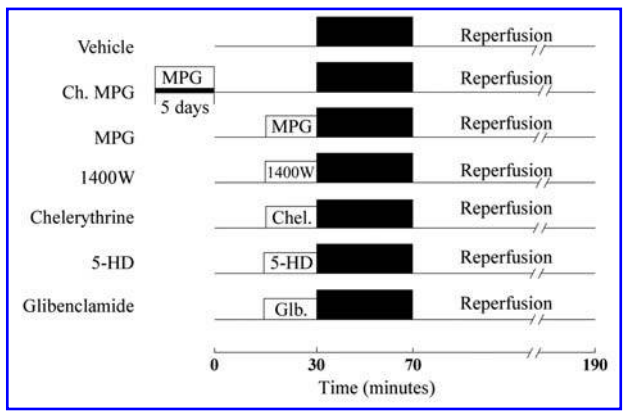

FIG. 1. Experimental protocol. Isolated and perfused BIOF1B hamster and BIO14.6 hamster hearts were subjected to 40 min of global ischemia followed by 120 min of reperfusion. Vehicle: BIOF1B and BIO14.6 hamsters were treated (i.p.) with 0.2 ml PBS for 5 days, and the isolated hearts were treated with dimethylsulfoxide (0.01%). Ch. MPG: BIOF1B and BIO14.6 hamsters were treated (i.p.) daily with 100 mg/kg *N*-(2-mercaptopropionyl)-glycine dissolved in 0.2 ml PBS for 5 days. MPG, 1400W, Chelerythrine (Chel.), 5-hydroxydecanoate (5-HD), and glibenclamide (Glb.): isolated and perfused BIOF1B and BIO14.6 hamster hearts were treated with 0.3 m*M* MPG, 10 m*M* 1400W, 5 μ*M* chelerythrine, 0.5 m*M* 5-HD or 10 μ*M* glibenclamide for 15 min before ischemia.

glibenclamide for 15 min just before ischemia. The vehicle and the chronic MPG groups of hearts were treated with 0.01% DMSO for 15 min just before ischemia.

Immunohistochemistry

After stabilization of the heart under Langendorff's perfusion, the heart was removed from the apparatus, and a 2-mm-thick of the midventricular slice was frozen with an O.C.T. compound (Tissue-Tek; Sakura, Tokyo, Japan) in liquid nitrogen for immunohistochemical analysis of iNOS. The frozen sections of 6 μm thick were fixed in acetone for 10 min at room temperature. Slides were incubated with a rabbit polyclonal iNOS antibody (Santa Cruz Biotechnology, Santa Cruz, CA) diluted 1:300 in PBS containing 1% bovine serum albumin (BSA) for 60 min at room temperature. Subsequently, slides were incubated with fluorescein isothiocyanate–conjugated goat anti-rabbit immunoglobulin (Ig; 1:200) for 60 min at room temperature. Nuclei were stained with propidium iodide (2 μg/ml). Immunofluorescence images were obtained by confocal laser microscopy (Olympus, Tokyo, Japan).

Immunoblot analysis

For immunoblot analysis, the heart was snap-frozen in liquid nitrogen, and the frozen tissues were homogenized with a lysis buffer containing 30 m*M* Tris, pH 7.4, 150 m*M* NaCl, 1% NP-40, 0.25% sodium deoxycholate, 1 m*M* EDTA, 0.1 m*M* phenylmethylsulfonyl fluoride, and a protease inhibitor cocktail Complete (Roche Diagnostics, Mannheim, Germany). The protein concentration was determined with a Bio-Rad protein assay (Bio-Rad Laboratories, Hercules, CA). The lysate samples were separated by a 7.5% sodium dodecylsulfate–polyacrylamide gel electrophoresis (SDS-PAGE), and the separated proteins were transferred to a polyvinylidene-difluoride membrane with a transfer buffer containing 25 m*M* Tris, 192 m*M* glycine, and 10% methanol. The membranes were blocked with 5% skimmed milk and immunoblotted with the anti-iNOS or rabbit polyclonal anti-nitrotyrosine (NT) antibodies (Cell Signaling, Beverly, MA). The blots were incubated with a peroxidase-conjugated goat anti-rabbit antibody and developed by using an enhanced chemiluminescence detection system (Amersham Biosciences, Tokyo, Japan), according to the manufacturer's instructions. 3-NT was detected as a 30-kDa band. The immunolabeling was quantified with a densitometric analysis by using Win Roof. Consistency in the data analysis was ensured by normalization of each immunoblot signal to the corresponding Coomassie Blue stain signal, as described previously (23).

iNOS activity assay

iNOS activity assay was performed as described (41). In brief, the frozen heart tissues were homogenized in 4 volumes of buffer containing 10 m*M* HEPES, pH 7.2, 0.32 *M* sucrose, 0.1 m*M* EDTA, 1m*M* dithiothreitol (DTT), and the protease inhibitor cocktail. The homogenate was centrifuged, and aliquots of the supernatant were incubated for 60 min at 37°C with (a) assay cocktail containing 50 m*M* L-valine, 1 m*M* DTT, 0.1 m*M* NADPH, 0.1 m*M* BH_4, 1 m*M* L-citrulline, 18 μ*M* L-arginine, 2 μ*M* L-[^{14}C]arginine, 1 m*M* $MgCl_2$, and 0.2 m*M* $CaCl_2$ in 50 m*M* KH_2PO_4, pH 7.2; (b) cocktail plus 1 m*M* EGTA; or (c) cocktail plus 1 m*M* EGTA plus 1 m*M* L-NMMA, to determine the total and Ca^{2+}-independent NOS (iNOS) activity. NOS activity was quantified by measuring L-[^{14}C]citrulline with a liquid scintillation counter after removal of untreated L-[^{14}C]arginine with 50W-X8 Dowex resin (Muromachi Technos Co., Tokyo, Japan).

PKC-ϵ activity assay

The phosphorylation activity of PKC-ϵ was measured as described (12). In brief, 50 μg proteins from the particulate fraction of the ventricular myocardium were immunoprecipitated overnight with rabbit polyclonal PKC-ϵ antibodies (Santa Cruz). The immunoprecipitates were subjected to a phosphorylation activity assay by using a PKC assay kit (Upstate Biotechnology).

Creatine kinase release

Creatine kinase (CK) release was measured as described previously (23).

Infarct-size measurements

Infarct-size measurements were performed by a triphenyltetrazolium chloride (TTC) staining method, as described (17).

Statistical analysis

All numeric data are expressed as mean ± SEM. Statistical analysis of data within and between groups was performed with one-way analysis of variance (ANOVA) followed by the Bonferroni post hoc test or two-way repeated measures ANOVA when comparisons were made at different time points.

RESULTS

Baseline morphologic characteristics of BIO14.6 hamster heart

It has been demonstrated that the earliest biologic and morphologic evidence of cardiomyopathy in BIO14.6 hamsters develops at 30–40 days of age (15). Increase in myocardial fibrosis and myocardial hypertrophy may affect postischemic LV function and infarct size. However, gross morphology, heart weight/body weight (Fig. 2A), and the area of fibrosis (Fig. 2B) were not significantly different between BIOF1B and BIO14.6 hamster hearts at 6 weeks of age. Moreover, echocardiography demonstrated no significant difference in systolic and diastolic LV diameters and LV ejection fraction between these hamsters (Fig. 2C). No visible infarction was detected at baseline by the TTC staining method in both groups of hearts (not shown).

Effect of prolonged and preischemic treatment with MPG on expression of iNOS in BIO14.6 hamster heart

Immunoblot assay showed significantly increased expression of iNOS in BIO14.6 hamster heart at 6 weeks of age

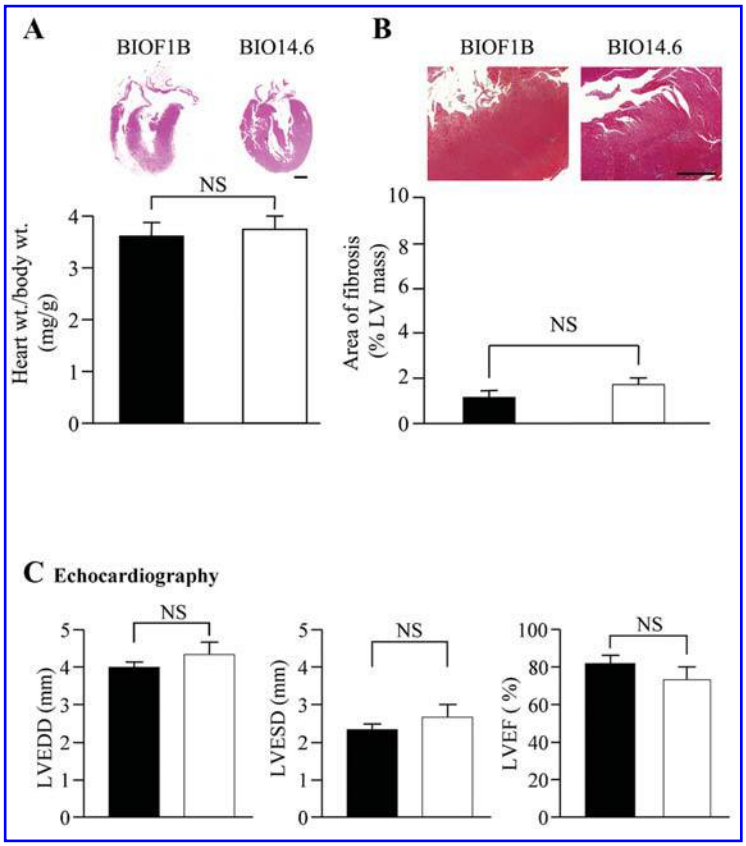

FIG. 2. Basic morphologic characteristics of BIOF1B and BIO14.6 hamster hearts. (**A**) Hematoxylin-eosin staining of the heart and heart weight/body weight ratio. (**B**) Masson trichrome staining of the heart and area of fibrosis. Bars indicate 1 mm. (**C**) Echocardiography. LVEDD, left ventricular end-diastolic diameter; LVESD, left ventricular end-systolic diameter; LVEF, left ventricular ejection fraction. Solid bar and open bar represent BIOF1B hamster and BIO14.6 hamster, respectively. Each bar graph represents mean ± SEM of five experiments. NS, not significant.

compared with the control hamster heart (Fig. 3A). Immunohistochemical studies showed increased iNOS expression in the cytoplasm of cardiomyocytes (Fig. 3B). Long-term treatment with MPG inhibited the cytoplasmic iNOS expression in BIO14.6 hamster heart.

Effect of prolonged and preischemic treatment with MPG on iNOS activity and NT formation in BIO14.6 hamster heart

Long-term treatment with MPG and brief treatment (15 min) with 1400W significantly inhibited activation of iNOS in

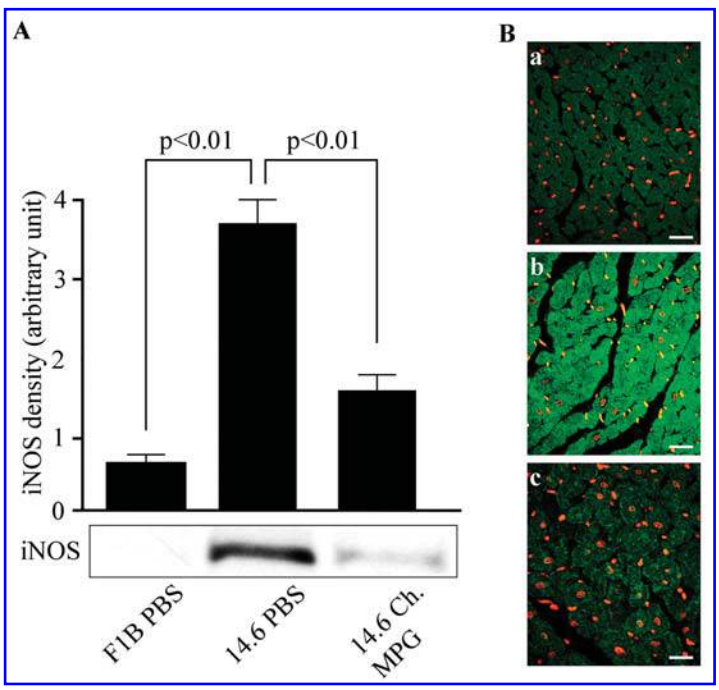

FIG. 3. iNOS expression. (**A**) Immunoblotting for iNOS protein in the heart. BIOF1B (F1B) and BIO14.6 (14.6) hamsters were treated with 0.2 ml PBS or 100 mg/kg *N*-(2-mercaptopropionyl)-glycine in 0.2 ml PBS for 5 days (Ch. MPG). Each bar graph represents mean ± SEM of five experiments. (**B**) Representative images of iNOS immunofluorescence. a, BIOF1B hamster treated (i.p) with PBS for 5 days; b, BIO14.6 hamster treated with PBS for 5 days; c, BIO14.6 hamster treated (i.p.) with MPG for 5 days. Bars indicate 20 μm.

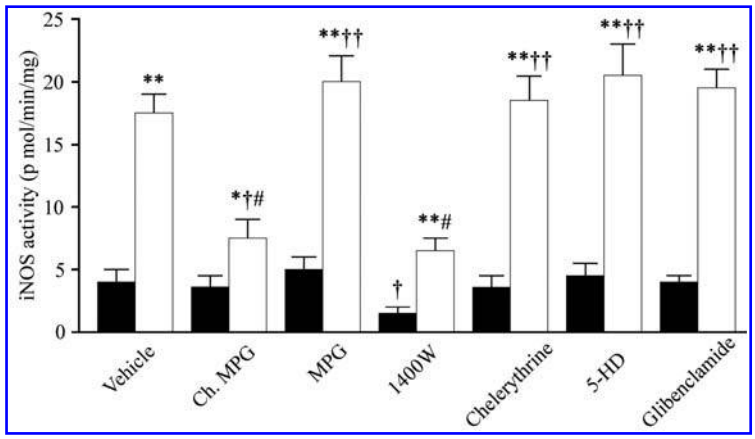

FIG. 4. iNOS activity assay. The experimental groups are shown in Fig. 1. Solid bars and open bars indicate BIOF1B and BIO14.6 hamster heart, respectively. Each bar graph represents mean ± SEM of five experiments. *$p < 0.05$, **$p < 0.01$ between BIOF1B and BIO14.6 hamster hearts in each treatment. †$p < 0.05$, ††$p < 0.01$ compared with BIOF1B hamster heart treated with the vehicle; #$p < 0.01$ between BIO14.6 hamster heart treated with the vehicle and BIO14.6 hamster heart treated with respective drugs.

BIO14.6 hamster heart (Fig. 4). However, brief treatment with MPG did not inhibit activation of iNOS. Similarly, iNOS activation was not inhibited by brief treatment with chelerythrine, 5-HD, and glibenclamide. Ca^{2+}-dependent NOS (cNOS; endothelial NOS, and/or neuronal NOS) activity was not different between the control and BIO14.6 hamster heart and was not affected by any treatments described earlier (not shown).

Formation of 3-NT is a marker of oxidative/nitrosative stress (18). Therefore, we measured 3-NT content in the hamster hearts. 3-NT was significantly increased in the vehicle-treated BIO14.6 hamster heart compared with the vehicle-treated control hamster heart (Fig. 5) but was inhibited by long-term as well as brief treatment with MPG. Treatment with 1400W also abolished 3-NT formation. However, treatment with chelerythrine, 5-HD, and glibenclamide had no significant effect on 3-NT formation. No significant change in 3-NT was noted by treatment with long-term as well as brief treatment with MPG or by brief treatment with 1400W, chelerythrine, 5-HD, and glibenclamide in the control hamster heart (not shown).

Prolonged and preischemic treatment with MPG inhibits activation of PKC-ϵ in BIO14.6 hamster heart

We measured PKC-ϵ activity as an index for cardioprotective signal transduction, because this PKC isoform has consistently been implicated in cardioprotection against I/R injury (7, 14, 32). PKC-ϵ activity was significantly higher in BIO14.6 hamster heart compared with the control hamster heart (Fig. 6). Activation of PKC-ϵ in BIO14.6 hamster heart was abolished by prolonged or preischemic treatment with MPG. Preischemic treatment with 1400W or chelerythrin also significantly inhibited activation of PKC-ϵ, although only chelerythrine significantly inhibited PKC-ϵ activity in the control hamster heart. Activation of PKC-ϵ in BIO14.6 hamster heart was not significantly inhibited by treatment with 5-HD or glibenclamide.

BIO14.6 hamster heart is tolerated to ischemia/reperfusion injury

CK release during reperfusion and infarct size 2 h after reperfusion were significantly smaller in BIO14.6 hamster heart compared with the control hamster heart (Table 1 and Fig. 7).

No significant difference was found in LV developed pressure (LVDP), LVEDP, heart rate, and coronary flow between the control and BIO14.6 hamster heart before ischemia (Tables 2 and 3). LVDP recovered to a nearly preischemic level 15 min after reperfusion in the control hamster heart but decreased as a function of time during reperfusion. LVEDP markedly increased 15 min after reperfusion and gradually decreased thereafter. Heart rate decreased immediately after

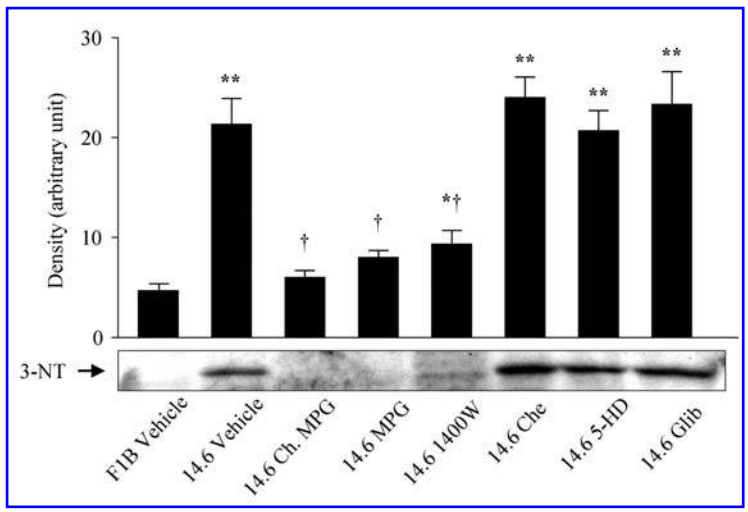

FIG. 5. Nitrotyrosine formation. 3-nitrotyrosine (3-NT) was detected and quantified as described in Methods. F1B, BIOF1B hamster; 14.6, BIO14.6 hamster. The experimental groups are shown in Fig. 1. Each bar graph represents mean ± SEM of five experiments. *$p < 0.05$, **$p < 0.01$ compared with BIOF1B hamster heart treated with the vehicle, †$p < 0.01$ compared with BIO14.6 hamster heart treated with the vehicle.

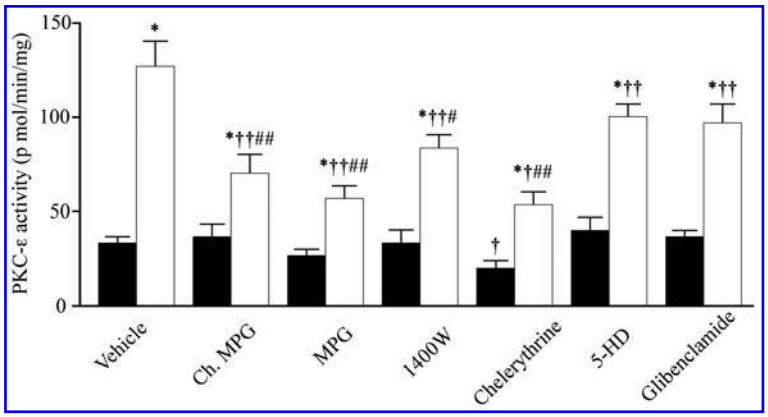

FIG. 6. Protein kinase C (PKC)-ϵ activity assay. The experimental groups are shown in Fig. 1. Solid bars and open bars indicate BIOF1B and BIO14.6 hamster hearts, respectively. Each bar graph represents mean ± SEM of five experiments. *$p < 0.01$ between BIOF1B and BIO14.6 hamster hearts in each treatment. †$p < 0.05$, ††$p < 0.01$ compared with BIOF1B hamster heart treated with the vehicle, #$p < 0.05$, ##$p < 0.01$ between BIO14.6 hamster heart treated with vehicle and BIO14.6 hamster heart treated with respective drugs.

reperfusion but increased between 15 and 60 min after reperfusion, although it did not reach the preischemic level. Coronary flow was completely restored 15 min after reperfusion but gradually decreased thereafter. In contrast to the control hamster heart, LVDP, LVEDP, heart rate, and coronary flow were returned to the preischemic level within 15 min after reperfusion and maintained at the same level during the rest of reperfusion in BIO14.6 hamster heart.

Prolonged treatment with MPG increases myocardial necrosis and decreases postischemic recovery of LV function in BIO14.6 hamster heart

Although long-term treatment with MPG had no significant effect on CK release and infarct size in the control hamster heart, the same treatment modality significantly increased infarct size in BIO14.6 hamster heart (Table 1 and Fig. 7).

Prolonged treatment with MPG had no significant effect on postischemic recovery of LV function and coronary flow in the control hamster heart. However, the same treatment modality significantly decreased recovery of LV function and coronary flow in BIO14.6 hamster heart.

Preischemic treatment with MPG differentially affects myocardial necrosis and postischemic LV function between the control and BIO14.6 hamster heart

Preischemic treatment with MPG significantly decreased CK release and infarct size in the control hamster heart (Table 1 and Fig. 7). In contrast, preischemic treatment with

TABLE 1. CREATINE KINASE (CK) RELEASE

			Reperfusion (min)				
	Baseline	*Preischemia*	*15*	*30*	*60*	*90*	*120*
CK release (IU/min/g)							
F1B-vehicle	0.0 ± 0.0	0.0 ± 0.0	3.5 ± 0.6	2.1 ± 0.4	0.7 ± 0.1	0.3 ± 0.1	0.2 ± 0.0
14.6-vehicle	0.0 ± 0.0	0.0 ± 0.0	0.5 ± 0.1[b]	0.3 ± 0.1[b]	0.2 ± 0.1[b]	0.1 ± 0.0[a]	0.1 ± 0.0[a]
F1B-Ch. MPG	0.0 ± 0.0	0.0 ± 0.0	3.5 ± 0.6	2.0 ± 0.3	0.8 ± 0.1	0.3 ± 0.1	0.3 ± 0.2
14.6-Ch. MPG	0.0 ± 0.0	0.0 ± 0.0	2.6 ± 0.4[e]	1.3 ± 0.3[e]	0.5 ± 0.1[e]	0.2 ± 0.0	0.1 ± 0.0
F1B-MPG	0.0 ± 0.0	0.0 ± 0.0	2.3 ± 0.3	1.1 ± 0.3[c]	0.5 ± 0.1	0.2 ± 0.1	0.2 ± 0.0
14.6-Ch. MPG	0.0 ± 0.0	0.0 ± 0.0	1.9 ± 0.2[c,e]	0.8 ± 0.1[c,d]	0.3 ± 0.1[c]	0.1 ± 0.0[c]	0.1 ± 0.0
F1B-1400W	0.0 ± 0.0	0.0 ± 0.0	3.2 ± 0.3	2.1 ± 0.4	0.6 ± 0.1	0.3 ± 0.1	0.2 ± 0.0
14.6-1400W	0.0 ± 0.0	0.0 ± 0.0	2.5 ± 0.3[e]	1.2 ± 0.3[c]	0.4 ± 0.0[c,e]	0.1 ± 0.1	0.1 ± 0.0
F1B-Chel.	0.0 ± 0.0	0.0 ± 0.0	3.9 ± 0.5	2.4 ± 0.4	0.8 ± 0.1	0.3 ± 0.1	0.2 ± 0.1
14.6-Chel.	0.1 ± 0.0	0.0 ± 0.0	2.8 ± 0.4[e]	1.5 ± 0.3[e]	0.7 ± 0.2[e]	0.2 ± 0.0	0.2 ± 0.1
F1B-5-HD	0.0 ± 0.0	0.0 ± 0.0	3.3 ± 0.2	2.0 ± 0.3	0.6 ± 0.1	0.2 ± 0.1	0.1 ± 0.1
14.6-5-HD	0.0 ± 0.0	0.1 ± 0.0	2.2 ± 0.3[c,e]	1.4 ± 0.3[e]	0.4 ± 0.1[e]	0.2 ± 0.0[d]	0.1 ± 0.0
F1B-Glb.	0.0 ± 0.0	0.0 ± 0.0	3.4 ± 0.7	1.8 ± 0.2	0.6 ± 0.1	0.2 ± 0.1	0.1 ± 0.1
14.6-Glb.	0.1 ± 0.0	0.0 ± 0.0	2.1 ± 0.5	1.2 ± 0.2[c,e]	0.5 ± 0.1[e]	0.1 ± 0.1	0.1 ± 0.0

Experimental protocol is shown in Fig. 1. MPG, 2-mercaptopropionylglycine; Chel, chelerythrine; 5-HD, 5-hydroxy decanoic acid; Glb, glibenclamide.

Data are expressed as mean ± SEM of five experiments. F1B, BIOF1B hamster; 14.6, BIO14.6 hamster [a]$p < 0.05$, [b]$p<0.01$ between F1B and 14.6. [c]$p<0.05$ compared to F1B-vehicle. [d]$p<0.05$, [e]$p<0.01$ compared to 14.6-vehicle.

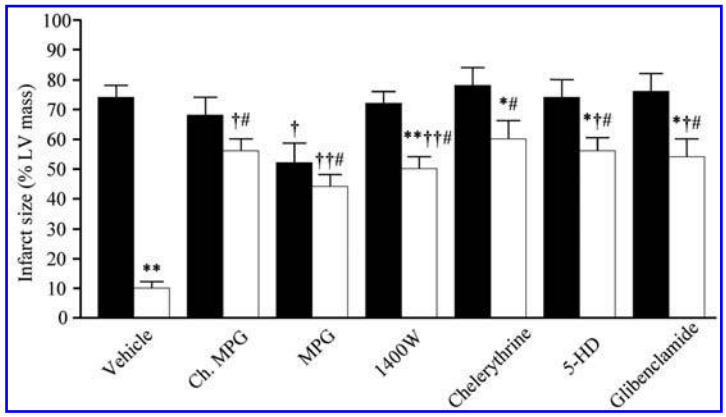

FIG. 7. Infarct size. The experimental groups are shown in Fig. 1. Solid bars and open bars indicate BIOF1B and BIO14.6 hamster hearts, respectively. Each bar graph represents mean ± SEM of five experiments. *$p < 0.05$, **$p < 0.01$ between BIOF1B and BIO14.6 hamster hearts in each treatment. †$p < 0.05$, ††$p < 0.01$ compared with BIOF1B hamster heart treated with the vehicle, #$p < 0.01$ between BIO14.6 hamster heart treated with the vehicle and BIO14.6 hamster heart treated with respective drugs.

MPG significantly increased CK release and infarct size in BIO14.6 hamster heart compared with the vehicle-treated BIO14.6 hamster heart.

Preischemic treatment with MPG significantly increased LVDP, heart rate, and coronary flow and decreased LVEDP during reperfusion in the control hamster heart (Tables 2 and 3). In contrast, preischemic treatment with MPG significantly decreased LVDP and heart rate and significantly increased LVEDP in BIO14.6 hamster heart.

Preischemic treatment with 1400W, chelerythrine, 5-HD, and glibenclamide increases myocardial necrosis and decreases postischemic recovery of LV function in BIO14.6 hamster heart

Preischemic treatment with 1400W, chelerythrine, 5-HD, and glibenclamide had no significant effect on CK release and infarct size in the control hamster heart but significantly increased CK release and infarct size in BIO14.6 hamster heart (Fig. 7).

These treatments also significantly decreased LVDP, heart rate, and coronary flow and increased LVEDP during reperfusion in BIO14.6 hamster heart (Tables 2 and 3).

DISCUSSION

We investigated the role of oxidative/nitrosative stress in the tolerance to I/R injury in BIO14.6 hamster heart. Major findings of the present study were (a) BIO14.6 hamster hearts at 6 weeks of age had no significant morphologic change and hemodynamic deterioration, (b) these hamster hearts showed increased expression and activity of iNOS and increased NT formation, (c) when BIO14.6 hamster hearts were isolated and subjected to 40 min of global ischemia, these hearts showed smaller myocardial necrosis and greater recovery of LV function during reperfusion compared with the control hamster hearts, (d) long-term treatment with MPG inhibited upregulation of iNOS, NT formation, and activation of PKC-ϵ and eliminated the tolerance to I/R injury in BIO14.6 hamster heart, (e) preischemic brief treatment with MPG reduced myocardial necrosis and improved LV function during reperfusion in the control hamster heart, whereas the same treatment inhibited NT formation and activation of PKC-ϵ before ischemia without affecting iNOS activity and blocked the tolerance to I/R injury in BIO14.6 hamster heart, (f) preischemic brief treatment with 1400W inhibited iNOS activity, NT formation, and activation of PKC-ϵ and blocked the tolerance to I/R injury in BIO14.6 hamster heart, (g) preischemic brief treatment with chelerythrine inhibited activation of PKC-ϵ without affecting iNOS activity and NT formation and abrogated the tolerance to I/R injury in BIO14.6 hamster heart, and (h) preischemic brief treatment with 5-HD and glibenclamide had no effect on iNOS activity, NT formation and activation of PKC-ϵ but abrogated the tolerance to I/R injury in BIO14.6 hamster heart. These results suggest that oxidative/nitrosative stress is generated in BIO14.6 hamster heart before development of heart failure and such stress confers the tolerance to I/R injury through the activation of PKC and the downstream effectors, K_{ATP} channels.

It has been shown that oxidative/nitrosative stress is required to trigger late preconditioning (8, 9). NO generated by the endothelial NOS via the formation of ROS activates PKC-ϵ, which activates transcriptional factors with resultant upregulation of iNOS, which plays an obligatory role in cardioprotection against I/R injury (2, 9, 38). However, the role of ROS in the mediator phase of late preconditioning has not been determined. The present study demonstrating that preischemic brief treatment with MPG abolished the tolerance to I/R injury without affecting iNOS activity and 1400W abolished iNOS activity and cardioprotection in BIO14.6 hamster heart indicates that cooperative interaction of ROS and NO, presumably through the formation of peroxynitrite, but not NO alone plays an essential role in the cardioprotective signal transduction mediating the tolerance to I/R injury.

PKC-ϵ has consistently been implicated in the cardioprotective signal transduction against I/R injury (7, 14, 32). In the sequence of events that oxidative/nitrosative stress mediate the tolerance to I/R injury in BIO14.6 hamster heart, we demonstrated that PKC-ϵ exists downstream of oxidative/nitrosative stress, because preischemic brief treatment with MPG or 1400W inhibited NT formation, activation of PKC-ϵ, and the tolerance to I/R injury, whereas chelerythrine abolished the tolerance to I/R injury without affecting iNOS activity and NT formation. Conversely, K_{ATP} channels are the downstream effectors of PKC, because two structurally distinct K_{ATP} channel inhibitors abolished the tolerance to I/R injury without affecting activation of PKC-ϵ.

Table 2. Left Ventricular Function

			Reperfusion (min)				
	Baseline	*PI*	*15*	*30*	*60*	*90*	*120*
LVDP (mm Hg)							
F1B-vehicle	95 ± 5	93 ± 5	82 ± 5	76 ± 4	58 ± 6	53 ± 6	50 ± 5
14.6-vehicle	89 ± 4	90 ± 4	86 ± 5	88 ± 5	89 ± 6[b]	87 ± 6[b]	87 ± 6[b]
F1B-Ch. MPG	97 ± 6	98 ± 6	81 ± 6	77 ± 4	57 ± 3	54 ± 2	50 ± 3
14.6-Ch. MPG	92 ± 5	92 ± 4	55 ± 5[b,d,f]	55 ± 4[b,d,f]	50 ± 3[a,f]	49 ± 3[f]	52 ± 3[f]
F1B-MPG	91 ± 7	96 ± 6	94 ± 5	90 ± 5	76 ± 5[c]	71 ± 5[c]	65 ± 4[c]
14.6-MPG	88 ± 3	91 ± 4	70 ± 5[a]	68 ± 5[a,e]	63 ± 4[f]	60 ± 4[f]	59 ± 5[f]
F1B-1400W	94 ± 4	94 ± 4	87 ± 5	72 ± 4	62 ± 5	60 ± 3	58 ± 3
14.6-1400W	87 ± 3	88 ± 4	65 ± 6[a,d,e]	58 ± 5[c,f]	53 ± 5[f]	53 ± 5[f]	54 ± 5[f]
F1B-Chel.	93 ± 3	98 ± 3	84 ± 5	75 ± 4	63 ± 3	61 ± 2	58 ± 2
14.6-Chel.	88 ± 2	90 ± 3	64 ± 4[a,c,e]	57 ± 5[a,c,f]	53 ± 3[f]	52 ± 3[f]	54 ± 3[f]
F1B-5-HD	92 ± 2	91 ± 3	81 ± 6	70 ± 3	63 ± 4	59 ± 4	54 ± 3
14.6-5-HD	86 ± 3	87 ± 3	57 ± 5[b,d,f]	59 ± 5[c,f]	57 ± 6[f]	55 ± 5[f]	57 ± 5[f]
F1B-Glb.	93 ± 3	93 ± 3	78 ± 5	73 ± 3	61 ± 5	57 ± 3	56 ± 4
14.6-G1b.	89 ± 3	87 ± 3	66 ± 4[c,e]	63 ± 5[e]	60 ± 5[f]	59 ± 5[f]	59 ± 4[f]
LVEDP (mm Hg)							
F1B-vehicle	7 ± 1	7 ± 1	57 ± 5	54 ± 5	44 ± 4	34 ± 4	30 ± 3
14.6-vehicle	7 ± 0	7 ± 0	7 ± 1[b]	7 ± 0[b]	7 ± 1[b]	7 ±1[b]	7 ± 1[b]
F1B-Ch. MPG	8 ± 1	8 ± 1	52 ± 6	50 ± 6	43 ± 4	33 ± 4	29 ± 4
14.6-Ch. MPG	8 ± 1	7 ± 1	48 ± 3[f]	45 ± 1[f]	37 ± 3[f]	34 ± 3[f]	31 ± 4[f]
F1B-MPG	8 ± 1	8 ± 1	44 ± 3[c]	42 ± 3[c]	33 ± 3[c]	25 ± 3	23 ± 2
14.6-MPG	8 ± 1	8 ± 1	37 ± 4[d,f]	34 ± 4[d,f]	28 ± 4[d,f]	24 ± 3[c,f]	22 ± 3[f]
F1B-1400W	7 ± 1	7 ± 1	50 ± 4	52 ± 5	40 ± 5	32 ± 4	30 ± 4
14.6-1400W	7 ± 1	7 ± 1	38 ± 4[a,d,f]	35 ± 4[a,d,f]	34 ± 4[f]	26 ± 3[f]	26 ± 3[f]
F1B-Chel.	7 ± 1	8 ± 1	58 ± 5	55 ± 5	46 ± 4	37 ± 5	33 ± 4
14.6-Chel.	8 ± 1	8 ± 1	45 ± 5[f]	43 ± 4[f]	40 ± 4[f]	35 ± 3[f]	31 ± 3[f]
F1B-5-HD	9 ± 0	8 ± 0	55 ± 6	55 ± 6	42 ± 4	34 ± 3	30 ± 3
14.6-5-HD	7 ± 1	7 ± 1	43 ± 3[c,f]	41 ± 3[a,c,f]	34 ± 3[f]	28 ± 3[f]	29 ± 3[f]
F1B-Glb.	7 ± 1	7 ± 1	56 ± 7	52 ± 6	45 ± 5	36 ± 4	32 ± 4
14.6-Glb.	8 ± 1	7 ± 0	40 ± 4[a,c,f]	37 ± 4[a,c,f]	31 ± 4[a,c,e]	27 ± 3[f]	25 ± 3[f]
HR (rpm)							
F1B-vehicle	375 ± 18	372 ± 17	223 ± 13	245 ± 14	269 ± 13	268 ± 15	267 ± 15
14.6-vehicle	368 ± 13	365 ± 13	353 ± 16[b]	365 ± 18[b]	361 ± 17[b]	363 ± 16[b]	365 ± 18[b]
F1B-Ch. MPG	377 ± 20	375 ± 17	248 ± 15	275 ± 18	276 ± 15	277 ± 13	280 ± 13
14.6-Ch. MPG	357 ± 19	355 ± 18	249 ± 13[f]	265 ± 17[f]	275 ± 16[f]	277 ± 13[f]	272 ± 13[f]
F1B-MPG	367 ± 23	367 ± 22	289 ± 14[c]	297 ± 12[c]	318 ± 14	312 ± 14	310 ± 15
14.6-MPG	344 ± 15	347 ± 13	278 ± 15[c,e]	298 ± 16[c,e]	305 ± 16	306 ± 16	304 ± 16
F1B-1400W	375 ± 20	377 ± 19	225 ± 16	247 ± 20	284 ± 23	279 ± 21	278 ± 22
14.6-1400W	348 ± 11	350 ± 12	286 ± 22[a,c,e]	304 ± 20[a,c]	312 ± 18	313 ± 20	311 ± 21
F1B-Chel.	379 ± 26	376 ± 25	222 ± 14	249 ± 16	281 ± 14	280 ± 13	277 ± 14
14.6-Chel.	351 ± 23	349 ± 26	264 ± 18[f]	279 ± 16[f]	284 ± 16[f]	284 ± 16[f]	279 ± 17[f]
F1B-5-HD	373 ± 19	374 ± 19	238 ± 16	259 ± 15	272 ± 15	297 ± 16	294 ± 13
14.6-5-HD	346 ± 22	348 ± 21	278 ± 14[c,e]	303 ± 13[c,e]	300 ± 12[e]	302 ± 11[e]	297 ± 11[e]
F1B-Glb.	370 ± 17	367 ± 16	237 ± 17	250 ± 19	279 ± 20	278 ± 19	275 ± 19
14.6-G1b.	352 ± 19	354 ± 20	290 ± 21[c,e]	300 ± 19[c,e]	299 ± 17[e]	299 ± 18[e]	297 ± 20[e]

Experimental protocol is shown in Fig. 1. F1B, BIOF1B hamster; 14.6, BIO14.6 hamster; MPG, 2-mercaptopropionylglycine; Chel, chelerythrine; 5-HD, 5-hydroxy decanoic acid; Glb, glibenclamide.

Data are expressed as mean ± SEM of five experiments. [a]$p<0.05$, [b]$p<0.01$ between F1B and 14.6. [c]$p<0.05$, [d]$p<0.01$ compared to F1B-vehicle. [e]$p<0.05$, [f]$p<0.01$ compared to 14.6-vehicle. LVDP, left ventricular developed pressure; LVEDP, left ventricular end-diastolic pressure; HR, heart rate, rpm (rate per minute).

Accumulating evidence suggests that mitochondrial and sarcolemmal K_{ATP} channels are the major effectors of cardioprotection mediated by activation of PKC-ϵ (20, 25, 29). It has been shown that mitochondrial and sarcolemmal K_{ATP} channels play a crucial role in cardioprotection by pharmacologic and ischemic preconditioning (11). Although it is difficult to address which K_{ATP} channels, mitochondria, or sarcolemma, play a principal role in the tolerance to I/R injury because no specific inhibitors of these channels are available at present, circumstantial evidence suggests that mitochondrial and sarcolemmal K_{ATP} channels act in parallel to mitigate lethal oxidative damage and Ca^{2+}-overload in mitochondria during I/R (6, 11). It has been

TABLE 3. CORONARY FLOW

			Reperfusion (min)				
	Baseline	*Preischemia*	*15*	*30*	*60*	*90*	*120*
Coronary flow (ml/min/g)							
F1B-vehicle	17.7 ± 1.5	17.4 ± 1.3	20.0 ± 1.4	17.2 ± 1.4	14.5 ± 1.2	12.2 ± 1.1	11.1 ± 1.0
14.6-vehicle	18.4 ± 1.6	18.6 ± 1.5	22.2 ± 1.8	19.3 ± 1.5	18.7 ± 1.4[a]	18.7 ± 1.4[b]	18.4 ± 1.4[b]
F1B-Ch. MPG	17.9 ± 1.5	17.5 ± 1.5	20.9 ± 1.6	17.4 ± 1.3	15.4 ± 1.2	13.2 ± 1.1	12.1 ± 1.0
14.6-Ch. MPG	18.0 ± 1.3	18.2 ± 1.3	20.9 ± 1.3	16.9 ± 1.2	14.3 ± 1.1[d]	14.1 ± 1.0[d]	13.6 ± 1.0[d]
F1B-MPG	18.1 ± 1.7	17.8 ± 1.6	22.6 ± 1.6	20.1 ± 1.6	18.5 ± 1.3[c]	15.9 ± 1.2[c]	15.0 ± 1.2[c]
14.6-MPG	17.3 ± 1.4	18.1 ± 1.5	22.1 ± 1.7	19.6 ± 1.3	17.4 ± 1.2	15.8 ± 1.1[c]	15.1 ± 1.0[c]
F1B-1400W	18.1 ± 1.8	18.1 ± 1.7	19.5 ± 1.5	16.0 ± 1.4	14.3 ± 1.2	12.1 ± 1.2	11.4 ± 1.3
146-1400W	18.7 ± 1.5	17.5 ± 1.5	20.4 ± 1.7	19.1 ± 1.4	17.6 ± 1.3	14.3 ± 1.3[c]	14.2 ± 1.1[c]
F1B-Chel.	17.8 ± 1.9	18.3 ± 2.0	21.5 ± 2.0	17.5 ± 2.0	15.5 ± 1.9	13.4 ± 1.8	12.3 ± 1.6
14.6-Chel.	17.9 ± 1.4	18.9 ± 1.5	21.5 ± 1.5	17.0 ± 1.5	14.1 ± 1.5[d]	12.2 ± 1.4[e]	12.2 ± 1.2[e]
F1B-5-HD	17.0 ± 1.5	16.9 ± 1.3	19.7 ± 1.5	15.2 ± 1.4	15.3 ± 1.5	12.9 ± 1.4	11.7 ± 1.4
14.6-5-HD	18.6 ± 2.1	18.8 ± 2.2	19.6 ± 1.2	16.4 ± 1.1	14.7 ± 1.0[d]	13.3 ± 1.5[d]	12.5 ± 1.3[e]
F1B-Glb.	17.2 ± 1.1	17.4 ± 1.1	19.0 ± 1.0	17.6 ± 1.2	14.9 ± 1.1	12.0 ± 1.0	10.8 ± 0.9
14.6-Glb.	19.2 ± 1.8	19.6 ± 1.8	19.3 ± 1.9	17.3 ± 1.9	14.9 ± 1.6	13.8 ± 1.5[d]	12.7 ± 1.5[e]

Experimental protocol is shown in Fig. 1. F1B, BIOF1B hamster; 14.6, BIO14.6 hamster; MPG, 2-mercaptopropionylglycine; Chel, chelerythrine; 5-HD, 5-hydroxy decanoic acid; Glb, glibenclamide.

Data are expressed as mean ± SEM of five experiments.

[a]$p < 0.05$, [b]$p < 0.01$ between F1B and 14.6. [c]$p < 0.05$ compared to F1B-vehicle. [d]$p < 0.05$, [e]$p < 0.01$ compared to 14.6-vehicle.

demonstrated that depolarization of mitochondrial membrane potential associated with opening of mitochondrial K_{ATP} channels decreases Ca^{2+} uptake (13). Sarcolemmal K_{ATP} channels also may prevent Ca^{2+} overload by shortening the action-potential duration and reducing the Ca^{2+} entry (6, 11). Another important mechanism for cardioprotection conferred by mitochondrial and sarcolemmal K_{ATP} channel activation is the prevention of lethal oxidative stress, because either hypoxic preconditioning or the mitochondrial K_{ATP} channel opener, pinacidil or diazoxide, attenuated oxidative stress and protected cardiomyocytes (1, 39). Taken together, the tolerance to I/R injury observed in BIO14.6 hamster heart is consistent with a paradigm of cardioprotection proposed by many ischemic and pharmacologic preconditioning studies, suggesting that mitochondrial and sarcolemmal K_{ATP} channel activation mediated by oxidative/ nitrosative stress feeds back to inhibit lethal oxidative stress and matrix Ca^{2+} overload in mitochondria (16).

It has been established that oxidative stress is a cause of I/R injury (30). In this experimental model, it appears that oxidative stress played an injurious role during I/R in the control hamster heart but not in BIO14.6 hamster heart. This observation suggests that BIO14.6 hamster heart is equipped with a defense system against lethal oxidative stress during I/R. The effect of prolonged exposure to oxidative stress on an antioxidative defense system is controversial. It has been demonstrated that long-term exposure to oxidative stress promotes activation of antioxidative defense enzymes in the failing hypertensive rat heart (8). In contrast, manganese superoxide dismutase activity was reduced in the failing human heart despite an increased messenger RNA (mRNA) level of this enzyme (36). Although we did not investigate the status of the antioxidative defense system in BIO14.6 hamster heart, it is reasonable to assume that the antioxidative defense system in this hamster heart acts to eliminate lethal oxidative damage during I/R, while leaving oxidative/nitrosative stress for the development of the cardioprotective signal transduction. Indeed, several potential mechanisms are envisioned to explain a distinct role of oxidative stress in lethal I/R injury and acquisition of tolerance to I/R injury. First, the source of ROS in triggering cardioprotection and mediating I/R injury is different. Because a cardioprotective signaling complex is primarily formed in the plasma membrane microdomain (40), ROS generated in the vicinity of the plasma membrane may specifically target the proteins involved in the cardioprotective signaling complex. In contrast to ROS that trigger the formation of cardioprotective signaling, many but not all studies have shown that injurious ROS generated during I/R are derived predominantly from mitochondria (5, 21). Collectively, it is suggested that a relatively small amount of ROS generated in a specific plasma-membrane domain promotes signaling cascades that prevent a catastrophic increase in mitochondria-derived ROS during I/R. The temporal and the spatial differences of ROS formation and the target molecules of ROS in mediating cardioprotection and I/R injury remain to be investigated.

The present study used BIO14.6 hamster lacking the δ-sarcoglycan gene (28). δ-Sarcoglycan is a component of dystrophin–glycoprotein complex that is involved in the maintenance of sarcolemmal integrity against mechanical stress. Thus, the lack of this protein expression may affect the extent of myocardial I/R injury that is critically mediated by the loss of sarcolemmal integrity (10). In addition, the isolated and perfused heart preparation does not reflect *in situ* cardiovascular function. This experimental model eliminates the effect of circulating neurohumoral factors and inflammatory cells that potentially affect the cardioprotective signal transduction in BIO14.6 hamster heart *in situ*. Thus, interpretation of the *ex vivo* findings must be cautious.

In conclusion, the isolated and perfused BIO14.6 hamster heart was markedly tolerant to I/R injury through the exposure to oxidative/nitrosative stress. Oxidative stress acts up-

stream and downstream of iNOS to mediate the tolerance to I/R injury. Oxidative stresses are involved in upregulating iNOS, whereas at a distal step, ROS in concert with iNOS-derived NO generates oxidative/nitrosative stress and activates PKC-ϵ, which activates the downstream effector, K_{ATP} channels localized in mitochondria and possibly in sarcolemma, to block I/R injury. Whether this schema of oxidative/nitrosative stress-mediated cardioprotective cascades in BIO14.6 hamster heart is a unifying mechanism for acquisition of tolerance to I/R injury under various pathologic cardiovascular conditions awaits further studies.

ACKNOWLEDGMENTS

This work was supported in part by Research Grant from the Ministry of Education, Science, and Culture of Japan and the Promotion and Mutual Aid Corporation for Private Schools of Japan.

ABBREVIATIONS

ANOVA, analysis of variance; BH_4, tetrahydrobiopterine; DMSO, dimethylsulfoxide; DTT, dithiothreitol; EDTA, ethylenediaminetetraacetic acid; EGTA, ethylene glycol-bis(2-aminoethyl-ester)-*N,N,N′,N′*-tetraacetic acid; HD, hydroxydecanoic acid; HEPES, *N*-(2-hydroxyethyl)piperazine-*N′*-2-ethanesulfonic acid; iNOS, inducible form of nitric oxide synthase; I/R, ischemia/reperfusion; K_{ATP}, ATP-sensitive potassium channel; KHB, Krebs–Henseleit bicarbonate; LV, left ventricle; LVDP, left ventricular developed pressure; LVEDP, left ventricular end-diastolic pressure; MPG, 2-mercaptopropionylglycine; NMMA, N^G-monomethyl-L-arginine; NO, nitric oxide; NT, nitrotyrosine; PBS, phosphate-buffered saline; PKC, protein kinase C; ROS, reactive oxygen species; SDS-PAGE, sodium dodecylsulfate–polyacrylamide gel electrophoresis; TTC, triphenyltetrazolium chloride.

REFERENCES

1. Akao M, Ohler A, O'Rourke B, and Marban E. Mitochondrial ATP-sensitive potassium channels inhibit apoptosis induced by oxidative stress in cardiac cells. *Circ Res* 88: 1267–1275, 2001.
2. Bolli R, Manchikalapudi S, Tang XL, Takano H, Qiu Y, Guo Y, Zhang Q, and Jadoon AK. The protective effect of late preconditioning against myocardial stunning in conscious rabbits is mediated by nitric oxide synthase: evidence that nitric oxide acts both as a trigger and as a mediator of the late phase of ischemic preconditioning. *Circ Res* 81: 1094–1107, 1997.
3. Bolli R. The late phase of preconditioning. *Circ Res* 87: 972–983, 2000.
4. Bolli R. Cardioprotective function of inducible nitric oxide synthase and role of nitric oxide in myocardial ischemia and preconditioning: An overview of a decade of research. *J Mol Cell Cardiol* 33: 1897–1918, 2001.
5. Chen Q, Vazquez EJ, Moghaddas S, Hoppel CL, and Lesnefsky EJ. Production of reactive oxygen species by mitochondria: Central role of complex III. *J Biol Chem* 278: 36027–36031, 2003.
6. Cohen MV, Baines CP, and Downey JM. Ischemic preconditioning: from adenosine receptor of KATP channel. *Annu Rev Physiol* 62: 79–109, 2000.
7. Cross HR, Murphy E, Bolli R, Ping P, and Steenbergen C. Expression of activated PKC epsilon (PKC epsilon) protects the ischemic heart, without attenuating ischemic H(+) production. *J Mol Cell Cardiol* 34: 361–367, 2002.
8. Csonka C, Pataki T, Kovacs P, Muller SL, Schroeter ML, Tosaki A, and Blasig IE. Effects of oxidative stress on the expression of antioxidative defense enzymes in spontaneously hypertensive rat hearts. *Free Radic Biol Med* 29: 612–619, 2000.
9. Dawn B and Bolli R. Role of nitric oxide in myocardial preconditioning. *Ann N Y Acad Sci* 962: 18–41, 2002.
10. Ganote C and Armstrong S. Ischaemia and the myocyte cytoskeleton: Review and speculation. *Cardiovasc Res* 27: 1387–1403, 1993.
11. Gross GJ and Fryer RM. Sarcolemmal versus mitochondrial ATP-sensitive K^+ channels and myocardial preconditioning. *Circ Res* 84: 973–979, 1999.
12. Hattori R, Otani H, Uchiyama T, Imamura H, Cui J, Maulik N, Cordis GA, Zhu L, and Das DK. Src tyrosine kinase is the trigger but not the mediator of ischemic preconditioning. *Am J Physiol Heart Circ Physiol* 281: H1066–H1074, 2001.
13. Holmuhamedov EL, Jovanovic S, Dzeja PP, Jovanovic A, and Terzic A. Mitochondrial ATP-sensitive K^+ channels modulate cardiac mitochondrial function. *Am J Physiol* 275: H1567–H1576, 1998.
14. Inagaki K, Hahn HS, Dorn GW 2nd, and Mochly-Rosen D. Additive protection of the ischemic heart ex vivo by combined treatment with delta-protein kinase C inhibitor and epsilon-protein kinase C activator. *Circulation* 108: 869–875, 2003.
15. Jasmin G and Proschek L. Hereditary polymyopathy and cardiomyopathy in the Syrian hamster. I. Progression of heart and skeletal muscle lesions in the UM-X7.1 line. *Muscle Nerve* 5: 20–25, 1982.
16. Juhaszova M, Zorov DB, Kim SH, Pepe S, Fu Q, Fishbein KW, Ziman BD, Wang S, Ytrehus K, Antos CL, Olson EN, and Sollott SJ. Glycogen synthase kinase-3β mediates convergence of protection signaling to inhibit the mitochondrial permeability transition pore. *J Clin Invest* 113: 1535–1549,2004.
17. Kido M, Otani H, Kyoi S, Sumida T, Fujiwara H, Okada T, and Imamura H. Ischemic preconditioning-mediated restoration of membrane dystrophin during reperfusion correlates with protection against contraction-induced myocardial injury. *Am J Physiol Heart Circ Physiol* 287: H81–H90, 2004.
18. Koeck T, Fu X, Hazen SL, Crabb JW, Stuehr DJ, and Aulak KS. Rapid and selective oxygen-regulated protein tyrosine denitration and nitration in mitochondria. *J Biol Chem* 279: 27257–27262, 2004.
19. Kuzuya T, Hoshida S, Yamashita N, Fuji H, Oe H, Hori M, Kamada T, and Tada M. Delayed effects of sublethal ischemia on the acquisition of tolerance to ischemia. *Circ Res* 72: 1293–1299, 1993.

20. Lawrence KM, Townsend PA, Davidson SM, Carroll CJ, Eaton S, Hubank M, Knight RA, Stephanou A, and Latchman DS. The cardioprotective effect of urocortin during ischaemia/reperfusion involves the prevention of mitochondrial damage. *Biochem Biophys Res Commun* 321: 479–486, 2004.
21. Levraut J, Iwase H, Shao ZH, Vanden Hoek TL, and Schumacker PT. Cell death during ischemia: Relationship to mitochondrial depolarization and ROS generation. *Am J Physiol Heart Circ Physiol* 284: H549–H558, 2003.
22. Lopez Farre A and Casado S. Heart failure, redox alterations, and endothelial dysfunction. *Hypertension* 38: 1400–1405, 2001.
23. Lu K, Otani H, Yamamura T, Nakao Y, Hattori R, Ninomiya H, Osako M, and Imamura H. Protein kinase C isoform-dependent myocardial protection by ischemic preconditioning and potassium cardioplegia. *J Thorac Cardiovasc Surg* 121:137–148, 2001.
24. Marber MS, Latchman DS, Walker JM, and Yellon DM. Cardiac stress protein elevation 24 hours after brief ischemia or heat stress is associated with resistance to myocardial infarction. *Circulation* 88: 1264–1272, 1993.
25. Moon CH, Kim MY, Kim MJ, Kim MH, Lee S, Yi KY, Yoo SE, Lee DH, Lim H, Kim HS, Lee SH, Baik EJ, and Jung YS. KR-31378, a novel benzopyran analog, attenuates hypoxia-induced cell death via mitochondrial KATP channel and protein kinase C-epsilon in heart-derived H9c2 cells. *Eur J Pharmacol* 506: 27–35, 2004.
26. Murphy E. Primary and secondary signaling pathways in early preconditioning that converge on the mitochondria to produce cardioprotection. *Circ Res* 94: 7–16, 2004.
27. Murry CE, Jennings RB, and Reimer KA. Preconditioning with ischemia: A delay of lethal cell injury in ischemic myocardium. *Circulation* 74: 1124–1136, 1986.
28. Nigro V, Okazaki Y, Belsito A, Piluso G, Matsuda Y, Politano L, Nigro G, Ventura C, Abbondanza C, Molinari AM, Acampora D, Nishimura M, Hayashizaki Y, and Puca GA. Identification of the Syrian hamster cardiomyopathy gene. *Hum Mol Genet* 6: 601–607, 1997.
29. Ohnuma Y, Miura T, Miki T, Tanno M, Kuno A, Tsuchida A, and Shimamoto K. Opening of mitochondrial K(ATP) channel occurs downstream of PKC-epsilon activation in the mechanism of preconditioning. *Am J Physiol Heart Circ Physiol* 283: H440–H447, 2002.
30. Otani H. Reactive oxygen species as mediators of signal transduction in ischemic preconditioning. *Antioxid Redox Signal* 6: 449–469, 2004.
31. Pacher P, Schulz R, Liaudet L, and Szabo C. Nitrosative stress and pharmacological modulation of heart failure. *Trends Pharmacol Sci* 26: 302–310, 2005.
32. Ping P, Song C, Zhang J, Guo Y, Cao X, Li RC, Wu W, Vondriska TM, Pass JM, Tang XL, Pierce WM, and Bolli R. Formation of protein kinase C(epsilon)-Lck signaling modules confers cardioprotection. *J Clin Invest* 109: 499–507, 2002.
33. Qiu Y, Ping P, Tang XL, Manchikalapudi S, Rizvi A, Zhang J, Takano H, Wu WJ, Teschner S, and Bolli R. Direct evidence that protein kinase C plays an essential role in the development of late preconditioning against myocardial stunning in conscious rabbits and that epsilon is the isoform involved. *J Clin Invest* 101: 2182–2198, 1998.
34. Sabri A, Hughie HH, and Lucchesi PA. Regulation of hypertrophic and apoptotic signaling pathways by reactive oxygen species in cardiac myocytes. *Antioxid Redox Signal* 5: 731–740, 2003.
35. Sadoshima J, Montagne O, Wang Q, Wang G, Warden J, Liu J, Takagi G, Karoor V, Hong C, Johnson GL, Vatner DE, and Vatner SF. The MEKK1-JNK pathway plays a protective role in pressure overload but does not mediate cardiac hypertrophy. *J Clin Invest* 110: 271–279, 2002.
36. Sam F, Kerstetter DL, Pimental DR, Mulukutla S, Tabaee A, Bristow MR, Colucci WS, and Sawyer DB. Increased reactive oxygen species production and functional alterations in antioxidant enzymes in human failing myocardium. *J Card Fail* 11: 473–480, 2005.
37. Takano H, Zou Y, Hasegawa H, Akazawa H, Nagai T, and Komuro I. Oxidative stress-induced signal transduction pathways in cardiac myocytes: Involvement of ROS in heart diseases. *Antioxid Redox Signal* 5: 789–794, 2003.
38. Tang XL, Takano H, Rizvi A, Turrens JF, Qiu Y, Wu W-J, Zhang Q, and Bolli R. Oxidant species trigger late preconditioning against myocardial stunning in conscious rabbits. *Am J Physiol Heart Circ Physiol* 282:H281–H291, 2002.
39. Vanden Hoek T, Becker LB, Shao ZH, Li CQ, and Schumacker PT. Preconditioning in cardiomyocytes protects by attenuating oxidant stress at reperfusion. *Circ Res* 86: 541–548, 2000.
40. Vondriska TM, Zhang J, Song C, Tang XL, Cao X, Baines CP, Pass JM, Wang S, Bolli R, and Ping P. Protein kinase C epsilon-Src modules direct signal transduction in nitric oxide-induced cardioprotection: Complex formation as a means for cardioprotective signaling. *Circ Res* 88: 1306–1313, 2001.
41. Wakeno-Takahashi M, Otani H, Nakao S, Imamura H, and Shingu K. Isoflurane induces second window of preconditioning through upregulation of inducible nitric oxide synthase in rat heart. *Am J Physiol Heart Circ Physiol* 289: H2585–H2591, 2005.

Address reprint requests to:
Hajime Otani, M.D.
Cardiovascular Center
Kansai Medical University
Moriguchi City, 570-8507
Japan

E-mail: otanih@takii.kmu.ac.jp

Date of first submission to ARS Central, December 19, 2005; date of acceptance, February 19, 2006.

This article has been cited by:

1. Juliana C. Fantinelli, Luisa F. González Arbeláez, Ignacio A. Pérez Núñez, Susana M. Mosca. 2012. Protective effects of N-(2-mercaptopropionyl)-glycine against ischemia–reperfusion injury in hypertrophied hearts. *Experimental and Molecular Pathology* . [CrossRef]
2. Alma Rus, Lourdes Castro, Maria Luisa del Moral, Ángeles Peinado. 2010. Inducible NOS inhibitor 1400W reduces hypoxia/re-oxygenation injury in rat lung. *Redox Report* **15**:4, 169-178. [CrossRef]
3. Hajime Otani . 2009. The Role of Nitric Oxide in Myocardial Repair and Remodeling. *Antioxidants & Redox Signaling* **11**:8, 1913-1928. [Abstract] [Full Text PDF] [Full Text PDF with Links]
4. Yu-si Cheng, De-zai Dai, Yin Dai. 2009. Isoproterenol disperses distribution of NADPH oxidase, MMP-9, and pPKC# in the heart, which are mitigated by endothelin receptor antagonist CPU0213. *Acta Pharmacologica Sinica* **30**:8, 1099-1106. [CrossRef]
5. Seiji Matsuhisa , Hajime Otani , Toru Okazaki , Koji Yamashita , Yuzo Akita , Daisuke Sato , Akira Moriguchi , Toshiji Iwasaka . 2008. N-Acetylcysteine Abolishes the Protective Effect of Losartan Against Left Ventricular Remodeling in Cardiomyopathy Hamster. *Antioxidants & Redox Signaling* **10**:12, 1999-2008. [Abstract] [Full Text PDF] [Full Text PDF with Links]
6. Hajime Otani . 2008. Ischemic Preconditioning: From Molecular Mechanisms to Therapeutic Opportunities. *Antioxidants & Redox Signaling* **10**:2, 207-248. [Citation] [Full Text PDF] [Full Text PDF with Links]